Available online at www.sciencedirect.com

ScienceDirect

Ceramics International 40 (2014) 2647–2653

CERAMICS INTERNATIONAL

www.elsevier.com/locate/ceramint

Microwave hydrothermal synthesis of Sr^{2+} doped ZnO crystallites with enhanced photocatalytic properties

Dan Li, Jian-Feng Huang*, Li-Yun Cao, Jia-Yin LI, Hai-Bo OuYang, Chun-Yan Yao

School of Material Science and Engineering, Shaanxi University of Science & Technology, Xi'an, Shaanxi 710021, PR China

Received 27 June 2013; received in revised form 15 October 2013; accepted 15 October 2013
Available online 22 October 2013

Abstract

Pure and Sr^{2+} doped ZnO crystallites were successfully synthesized via a microwave hydrothermal method using $Zn(NO_3)_2 \cdot 6H_2O$ and $Sr(NO_3)_2 \cdot 6H_2O$ as source materials. The phase and microstructure of the as-prepared $Zn_{1-x}Sr_xO$ crystallites were characterized by X-ray diffraction (XRD) and scanning electron microscopy (SEM). Ultraviolet–visible spectrum (UV–vis) and photochemical reaction instrument were used to analyze the photocatalytic properties of the particles. XRD results show that the diffraction peaks of the as-prepared $Zn_{1-x}Sr_xO$ crystallites shifted slightly toward lower 2θ angle with the increasing of Sr^{2+} doping concentration from 0% to 0.3%. The pure ZnO crystallites with lamellar structure are found transforming to a hexagonal columnar morphology with the increase of Sr^{2+} doping concentration. UV–vis analysis shows that the particles have a higher absorption in UV region with a slightly decreased of optical band (E_g) gap. The photocatalytic activity of Sr^{2+} doped ZnO crystallites was evaluated by the Rhodamine B (RhB) degradation in aqueous solution under visible-light irradiation. Compared with the pure ZnO particles, the photocatalytic properties of the Sr^{2+} doped ZnO crystallites are obviously improved. The photocatalysis experiment results demonstrate that the 0.1% Sr^{2+} doped ZnO exhibits the best photocatalytic activity for the degradation of Rhodamine B.

Keywords: A. Microwave processing; B. Defects; D. ZnO; Photocatalytic activity

1. Introduction

Zinc oxide (ZnO) is a semiconductor photocatalysis with a wide direct band gap (3.3 eV) and a high free-excition binding energy (60 meV) [1,2]. It is known as one of the important photocatalysts due to its advantages, including the large initial rates of activities, many active sites with high surface reactivity, low price and environmental safety [3,4]. However, it also presents some drawbacks like fast recombination rate of the photogenerated electron–hole pair and a low quantum yield in the photocatalytic reaction in aqueous solutions, highly restraining its photocatalytic activity under visible light [5–7]. Recently, how to enhance the photocatalytic activity of ZnO has drawn much attention from researchers all over the world. It is accepted that the surface area and lattice defects play important roles in photocatalytic activities of metal oxide semiconductors [8–10]. Researchers also found that doping is an effective and facile method to improve the photocatalytic properties because the variation of the surface area, the incorporation of dopant ions is able to generate lattice defects and variation of band gap energy [11,12]. Consequently, doping of transition metals, noble metals and non-metals is a very expedient way to improve the photocatalytic activity. Many elements such as Al [9], Ta [13], Cr [14], La [15], Ag [16] and I [17] have been used as dopants and showed better photocatalytic performance.

Alkaline earth metal ions can be taken as the candidate dopants to regulating and controlling the photocatalytic properties. Venkatachalam et al. [18] found that doping of TiO_2 nanoparticles with Mg^{2+} and Ba^{2+} produces higher photocatalytic activities than those of undoped TiO_2 nanoparticles or commercial TiO_2. Nevertheless, the entry of alkaline metal ions into the TiO_2 lattice also results in the creation of significant lattice defects because of the charge compensation and the ionic radius mismatch between Mg^{2+} (or Ba^{2+}) and Ti^{4+}, which may put huge uncertainties to the origin of photoactivities. It is well documented that ZnO is superior

*Corresponding author. Tel./fax: +86 29 86168802.
E-mail address: huangjfsust@126.com (J.-F. Huang).

0272-8842/$ - see front matter © 2013 Elsevier Ltd and Techna Group S.r.l. All rights reserved.
http://dx.doi.org/10.1016/j.ceramint.2013.10.061

semiconductor photocatalysis over TiO_2 in producing hydrogen peroxide, which allows its uses in efficient photodegradation of organic dye [19,20]. Hence, alkaline earth metal ions doped ZnO may also improve its photocatalytic properties greatly. Qiu et al. [21] prepared Mg^{2+} doped ZnO samples by a novel rheological phase reaction route and all $Zn_{1-x}Mg_xO$ samples exhibit high photoactivities comparable to pure ZnO by degrading methylene blue dye solution under UV light irradiation. Nevertheless, the research of alkaline earth metal ions doped ZnO to study its photocatalytic activity under visible-light irradiation has rarely been reported. As one of the important alkaline-earth metals, strontium is widely used for many applications including the electronics, metallurgy, chemical industry, military industry, optics and some other fields, it is also believed to be a good potential candidate material doped ZnO structures.

It is well known that ZnO crystallites can be doped with different ions through the hydrothermal method. Although the preparation of the doped ZnO has good optical performance via this method, but the conventional hydrothermal method usually costs long time and has more difficulties in technique [22–24]. Microwave-assisted hydrothermal (*M–H*) has been considered to be one of significant methods to prepare doped metal oxide crystallites in recent years. Microwaves energy has been demonstrated to enhance organic chemical reaction, increasing the net rate early in the heating process. This method could be attributed to the difficulties in controlling the simultaneous growth of the crystal and recombination of interparticles by the microwave heating [25–27].

In the present work, we try to use a novel microwave hydrothermal approach to prepare Sr^{2+} doped ZnO ($Zn_{1-x}Sr_xO$) crystallites and try to reveal their photocatalytic activity under visible-light irradiation.

2. Experimental

2.1. Source materials

The starting materials used in this experiment were analytical without further purification. Zinc nitrate hexahydrate ($Zn(NO_3)_2 \cdot 6H_2O$) (analytical grade, Guangdong Guangghua Sci-Tech Co., Ltd.) and strontium nitrate ($Sr(NO_3)_2$) (analytical grade, Sinopharm Chemical Reagent Co., Ltd.) were used as zinc and strontium sources, respectively. Sodium hydroxide (NaOH) (analytical grade) was purchased from Tianjing Hengxin Chemical Reagent Co., Ltd. Ethanol absolute (Tianjing Fuyu Industry of fine chemical Co., Ltd.).

2.2. Preparation of pure ZnO and Sr^{2+} doped ZnO

A typical synthesis route was as follows: firstly, 30 mL NaOH (3.2 mol/L) solution was slowly added into 30 mL $Zn(NO_3)_2 \cdot 6H_2O$ (1.6 mol/L) solution, the $Zn(OH)_2$ precipitation was obtained. This solution was then transferred to a Teflon-lined autoclave of 50 mL capacity to be put into a MDS-10 Microwave Hydrothermal System (Shanghai Sineo Microwave chemistry Co., Ltd.) and heated at 160 °C for 30 min. After the reaction was terminated and cooled down to room temperature, the as-prepared white precipitate was collected by filtration and purified by washing in deionized water and absolute ethyl alcohol for five times. Finally, the white precipitate was dried at 60 °C in a drying cabinet for 2 h to obtain the pure ZnO crystallites.

For the preparation of Sr^{2+} doped ZnO materials, different concentrations of $Sr(NO_3)_2$ with Sr^{2+} from 0.1% to 0.3% were put into 30 mL $Zn(NO_3)_2 \cdot 6H_2O$ (1.6 mol/L) solution separately. The rest steps of the preparation remain as the same as that of pure ZnO crystallites introduced above.

2.3. Characterization

The powder X-ray diffraction patterns of as-prepared samples were measured with an X-ray diffractometer (XRD, D/max-2200PC, Rigaku, Japan) with Cu K_α radiation at a scanning rate of 8 deg min^{-1} in the 2θ range from 15° to 70°. The surface morphology was observed with a Scanning Electron Microscopy (SEM, HITACHI Japan). UV–vis spectra were obtained on a Lambda 950 spectrophotometer (Perkin-Elmer, USA).

2.4. Measurement of photocatalytic activity

Photocatalytic performance test was carried out by employing BL-GHX-V photocatalytic reactor (Xi'an, BILOBN, Co., Ltd.) with xenon lamp (1000 W) used as the visible-light source. Fifty milligrams $Zn_{1-x}Sr_xO$ powders were added into 50 mL Rhodamine B (RhB) aqueous solution (10 mg/L) and dispersed under ultrasonic vibration for 10 min. The obtained suspension was continuously stirred 30 min in darkness to ensure the establishment of an adsorption–desorption equilibrium between the powder and the RhB molecules. Then the visible light was turned on to start the photocatalytic reaction. Five milliliters of the mixture were withdrawn and separated by centrifuging to remove any suspended solids at intervals of 30 min. The degradation process was monitored by an UV–vis absorption spectrometer (measuring the absorption of RhB at 554 nm). From the adsorption experiments, the percentage of RhB adsorbed on the catalyst surface was determined from the following equation:

$$\text{Percentageofadsorption} = (C_0 - C_t)/C_0 \times 100\% \quad (1)$$

Where C_0 represents the initial concentration of RhB and C_t represents the concentration of RhB after '*t*' minutes of visible light irradiation.

3. Results and discussion

3.1. XRD patterns of $Zn_{1-x}Sr_xO$

In order to investigate the crystal structure lattice parameters of the Sr^{2+} doped ZnO crystallites, XRD analysis is used. Fig. 1 shows the XRD patterns of pure ZnO and Sr^{2+} doped ZnO crystallites. For the Sr^{2+} doped ZnO crystallites prepared by the microwave hydrothermal method, the XRD analysis showed that a secondary phase occurred in the XRD pattern when the Sr^{2+}

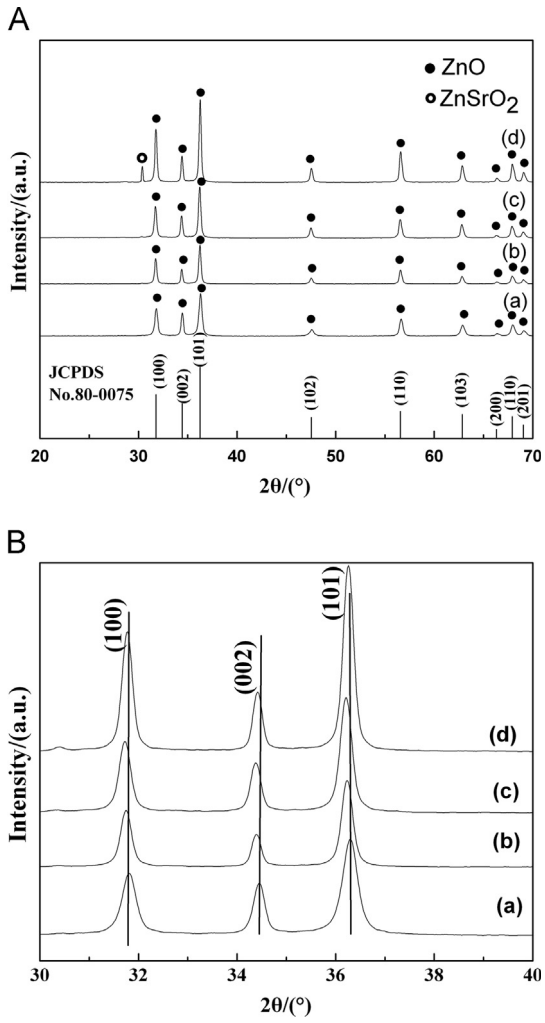

Fig. 1. (A) XRD patterns of the $Zn_{1-x}Sr_xO$ powders with different doping concentrations of Sr^{2+}, (B) enlarge figure of XRD, (a) $[Sr^{2+}]=0\%$, (b) $[Sr^{2+}]=0.1\%$, (c) $[Sr^{2+}]=0.2\%$, and (d) $[Sr^{2+}]=0.3\%$.

content is 0.3% (Fig.1A(d)). The major phase observed in the XRD pattern is the ZnO hexagonal wurtzite structure according to the JCPDS standard card number 36-1451 and the secondary phase observed in the XRD pattern is for $ZnSrO_2$. It shows that the Sr^{2+} doping concentration is excessive at 0.3%. Form the enlarged patterns given in Fig. 1(B), it can be found that all diffraction peaks of ZnO slightly shift toward lower 2θ angle, indicating the increase in crystallites parameters. This may result from the substitute of Zn^{2+} (ionic radius is 0.74 Å) by Sr^{2+} (ionic radius is 2.45 Å), which can be inferred that the Sr^{2+} ions have been infiltrated into the lattice of ZnO crystallites. When the peak intensities of (100) and (101) planes are compared, it can be further concluded that the doping of Sr^{2+} into ZnO crystal structure could also improve the crystallization of ZnO, which may result in the change of the unit cell parameter, crystallites size and active defect sites in ZnO [28].

3.2. SEM images of $Zn_{1-x}Sr_xO$

SEM surface images of the samples are shown in Fig. 2. As is shown in the Fig. 2(a), the structure of pure ZnO exhibited a lamellar-like structure with size ranges from 200 to 300 nm. This morphology was then found transformed into a granule-like structure with minimum size lower than 100 nm, which may cause stronger inner stress and lead to generation of more defects in the ZnO lattices when the Sr^{2+} doping concentration is set to 0.1% (Fig. 2(b)). With the increase of the Sr^{2+} doping concentration from 0.2% to 0.3% (Fig. 2(c) and (d)), the as-prepared ZnO shows a hexagonal columnar morphology finally. Based on the above observation, it can be concluded that the morphologies of Sr^{2+} doped ZnO are significantly different from the pure ZnO.

3.3. UV–vis absorption spectra and band gap analysis

The UV–vis absorption spectra of the prepared crystallites are shown in Fig. 3. It can be seen that there exists a strong absorption edge below 400 nm for all samples. With the increase of Sr^{2+} doped content, the absorption edge moves toward the high wavelength. Another significant and observable change locates the enhanced absorption in the visible-light region ranging from 400 to 700 nm for the Sr^{2+} doped ZnO (indicated by arrows), when compared with pure ZnO. This result can be attributed to the charge transfer between the ZnO valence or conduction band and the Sr^{2+} ion 5 s level [29]. This also proves that the Sr^{2+} ions are doped into the lattices of ZnO, which generates more active defect sites. As a result, more visible-light is absorbed via these active defect sites, which may lead to a higher photocatalytic activity of the doped ZnO crystallites in visible-light regions.

In order to determine the optical band gap energy (E_g) from the absorption spectra, a Tauc-plot analysis of the variation of the absorption coefficient (α) is employed by using the following equation:

$$\alpha = A(h\nu - E_g)^{1/2}/h\nu \quad (2)$$

Where E_g is the optical band gap of the samples, ν is the light frequency, h is the Plank constant and A is the proportionality coefficient [30]. Fig. 4 shows the plots of $(\alpha h\nu)^2$ versus $(h\nu)$ for the $Zn_{1-x}Sr_xO$ samples. Extrapolations of the linear portions of the plots onto the energy axis were used to estimate the values of E_g. Clearly, the band gap decreases slightly with the increase of Sr^{2+} doping concentrations. The shift of band gap may result from the change of ZnO lattice constant which will lead to the lattice distortion. It can generate more defects in the ZnO lattice and result in the change in absorption of light and the photocatalytic performance [31]. In addition, when the Sr^{2+} doping concentration reaches 0.1%, the ZnO exhibits the smallest band gap of 3.174 eV and the corresponding best absorption ability in visible-light region.

3.4. Photocatalytic activity of $Zn_{1-x}Sr_xO$

The photocatalytic activity of the as-prepared products is detected by the degradation of RhB under visible-light, as is shown in Fig. 5. The 30 min blank test shows that RhB is hardly decomposed without visible light irradiation. As can be seen from the Fig. 5(A), the Sr^{2+} doping ZnO exhibits higher photocatalytic activity than that of pure ZnO. When the Sr^{2+}

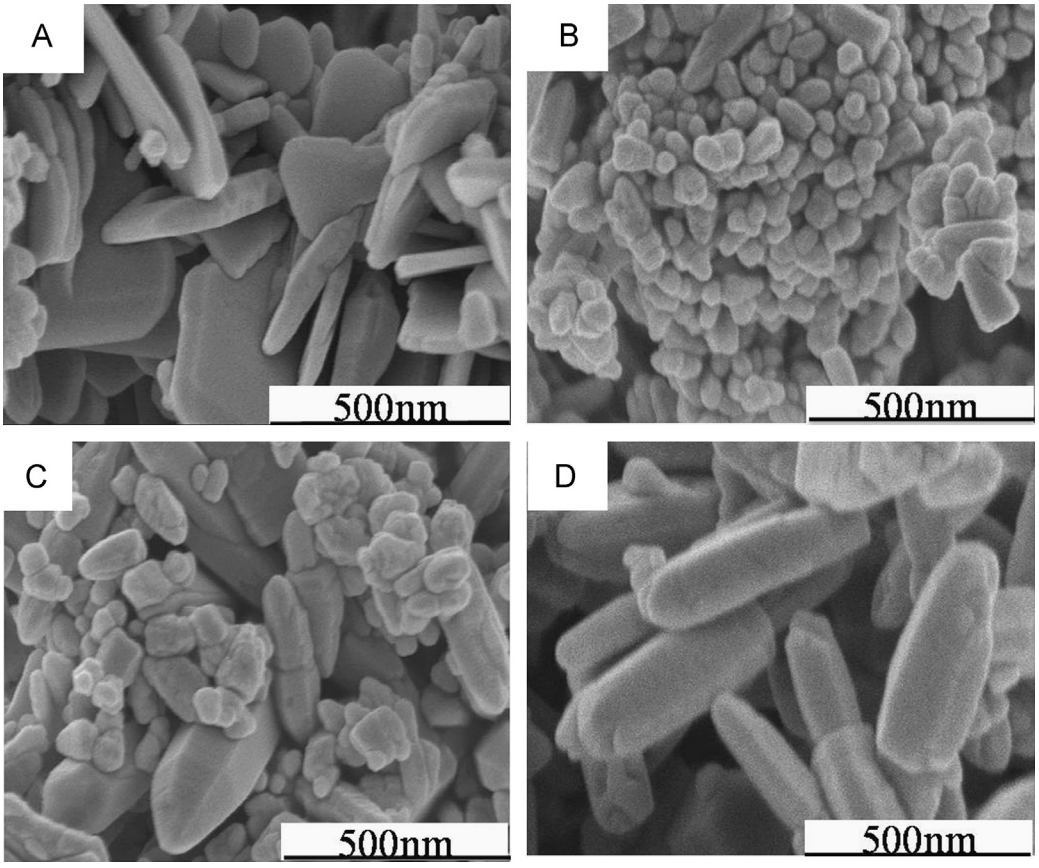

Fig. 2. SEM images of the $Zn_{1-x}Sr_xO$ powders with different doping concentrations of Sr^{2+}. (a) $[Sr^{2+}]=0\%$, (b) $[Sr^{2+}]=0.1\%$, (c)$[Sr^{2+}]=0.2\%$, and (d) $[Sr^{2+}]=0.3\%$.

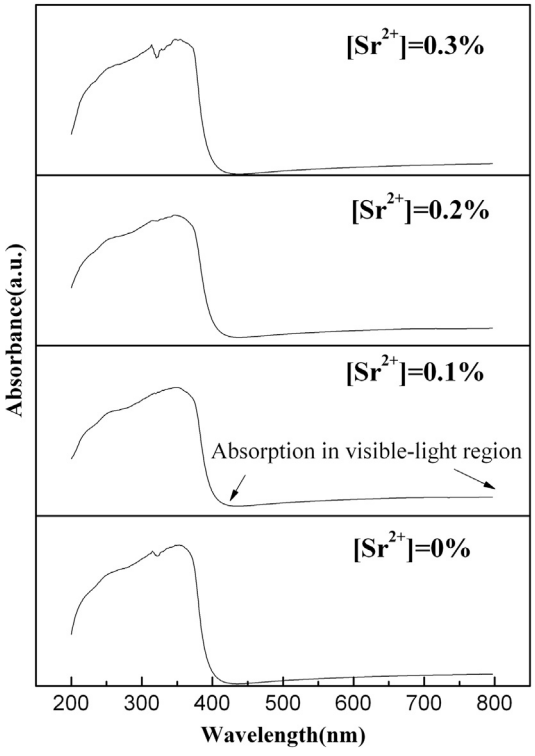

Fig. 3. UV–vis absorption spectra of the as-prepared $Zn_{1-x}Sr_xO$ powders with different doping concentrations of Sr^{2+}.

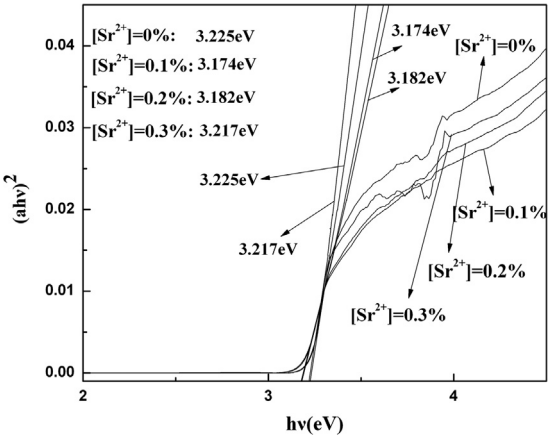

Fig. 4. The relationship between $(\alpha h\nu)^2$ and $h\nu$ of the $Zn_{1-x}Sr_xO$ powders with different doping concentrations of Sr^{2+}.

doping content exceeds 0.1%, the photocatalytic activity of the doped crystallites decreases with the increase of Sr^{2+} doped concentration. Hence, the order of the photocatalytic activities of the Sr^{2+} doped ZnO with different Sr^{2+} doping concentrations is as follows: $0.1\% > 0.2\% > 0.3\% > 0\%$. The 0.1% Sr^{2+} doped ZnO photocatalyst exhibits the highest photocatalytic decolorization efficiency with RhB concentration reduced by as much as 92% after 180 min irradiation. The

detailed results of the adsorption spectra during the photocatalytic degradation process of 0.1% Sr^{2+} doped ZnO are displayed in Fig. 5(B).

The above XRD, SEM and UV–vis absorption spectra analyses results reveal that when the Sr^{2+} doping content is 0.1%, compared with the pure ZnO and other Sr^{2+} doping content powders, it has the minimum particle size, more lattice defects, maximum specific surface areas, strongest absorption in the visible-light region and smallest band gap. These characteristics are beneficial for the improvement of photocatalytic activity. When the Sr^{2+} doped concentration further increased, better crystallization with increased particle size will lead to small specific surface area with narrowed absorption in the visible-light region and decreased active and valid defects for photodegradation. In addition, excessive Sr^{2+} ions may lead to the recombination of photogenerated electrons and holes, decreasing the photocatalytic activity of ZnO [32–38].

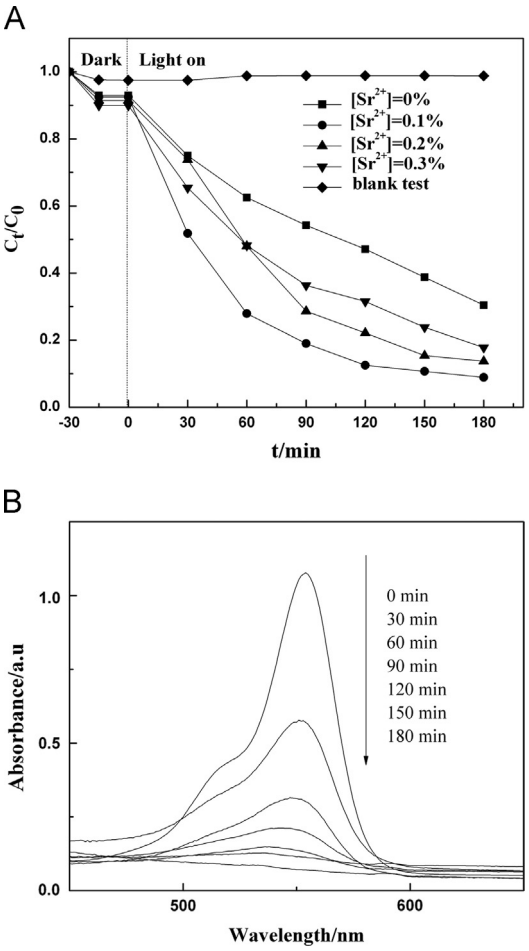

Fig. 5. (A) Photocatalytic properties of the $Zn_{1-x}Sr_xO$ powders with different doping concentrations of Sr^{2+}. (B) Visible-light spectral degradation of RhB by $Zn_{1-x}Sr_xO$ prepared at the Sr^{2+}-doping concentration of 0.1%.

To further understand how the defects improve the photocatalytic properties, the corresponding photocatalytic process needs discussing, which is represented in Fig. 6. When light with energy higher or equal to the band gap energy is irradiated to the semiconductor surface, a photo excited valence band electron is promoted to the conduction band, leaving behind a hole in the valence band to create electron–hole pairs. Then the defects benefit the efficient separation of the generation of the (e^-/h^+) pairs, which can lead to the formation of hydroxyl radicals (•OH) and superoxide radical anions (O_2^-). These radicals are the oxidizing species in the photocatalytic oxidation processes. During the photocatalytic process, the hydroxyl radical is recognized to be the most powerful oxidizing species which can attack organic pollutants at or near the surface of photocatalyst and make them into water and carbon dioxide. High charge separation rate is beneficial to form hydroxyl radical, which favors the decolorization of RhB. Based on the discussion mentioned above, it can be concluded that more active defect sites may provide much help to improve products' photocatalytic properties.

In this study, the Langmuir–Hinshelwood (L–H) model is used to describe the heterogeneous photocatalytic reaction between the $Zn_{1-x}Sr_xO$ crystallites and the RhB solution. The L–H kinetic equation is as follows [39]:

$$r = kK[C]/(1+K[C]) \quad (3)$$

Where r is the degration rate for RhB, K is the adsorption coefficient for RhB on the surface of the $Zn_{1-x}Sr_xO$ crystallites, k is the surface pseudo-first-order rate constant and C is the concentration of the RhB solution. If the adsorption coefficient on the surface of the $Zn_{1-x}Sr_xO$ crystallites is too small, so that $1 \gg K[C]$, and the L–H kinetic equation reduce to

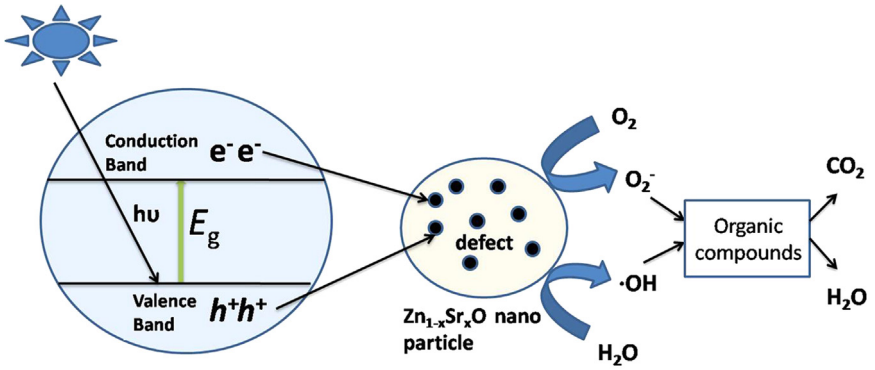

Fig. 6. Schematic representation of photocatalytic reaction in $Zn_{1-x}Sr_xO$ powders.

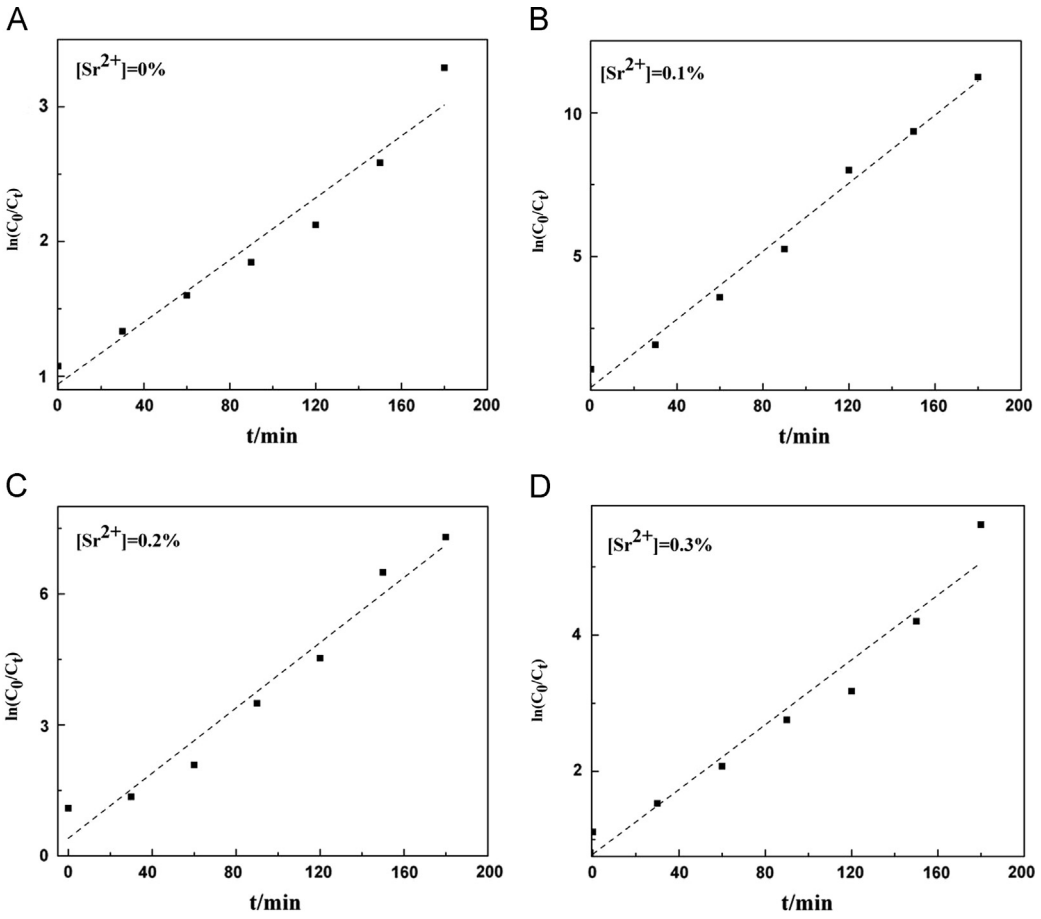

Fig. 7. Relationship between $\ln(C_0/C_t)$ and visible-light irradiation time of $Zn_{1-x}Sr_xO$ powders with different doping concentration of Sr^{2+}. (a) $[Sr^{2+}]=0\%$, (b) $[Sr^{2+}]=0.1\%$, (c)$[Sr^{2+}]=0.2\%$, and (d) $[Sr^{2+}]=0.3\%$.

the following simple first-order kinetic law:

$$\ln(C_0/C_t) = K_c t \quad (4)$$

Where K_c is the rate constant, C_0 and C_t represent initial equilibrium concentration of RhB and the reaction concentration of RhB, respectively.

Then the straight lines can be got by using regression fitting techniques, and their slopes correspond to the first-order kinetic rate constant (K_c), as is shown in Fig. 7. The calculated K_c, the corresponding first-order kinetic equation and the R^2 values are summarized in Table 1.

The fastest degradation rate for the decomposition of the RhB solution is obtained from the 0.1% Sr^{2+} doped ZnO crystallites when the ZnO crystallites were prepared by the microwave hydrothermal method. This can be explained by the more active centers of the powders.

Table 1
Parameter and linear kinetic equation of photocatalytic reaction.

Sr^{2+} (mol%)	K_c	First-order kinetic equation	R^2
0	0.01151	$0.01151t+0.00113$	0.94453
0.1	0.05918	$0.05918t+0.00301$	0.98468
0.2	0.03731	$0.03731t+0.0032$	0.95748
0.3	0.02377	$0.02377t+0.00235$	0.94389

4. Conclusion

ZnO crystallites were successfully doped with different amounts of Sr^{2+} via a microwave hydrothermal method. Results show that the increasing the doping concentration of Sr^{2+} led to the increase of ZnO crystal lattice with morphology change from lamellar-like into a hexagonal columnar structure. UV–vis results further present that these ZnO crystallites exhibit higher absorptions in visible-light region with decreased optical band gaps when increasing the Sr^{2+} doping concentration. Moreover, the Sr^{2+} doped ZnO crystallites are found to have enhanced photocatalytic activity than pure ZnO under visible-light irradiation. Our research suggests that Sr^{2+} doped ZnO crystallite may be a potential candidate for the practical application in photocatalytic degradation of organic contaminant.

Acknowledgments

This work has been supported by the National Natural Science Foundation of China (50942047), Innovation Team Assistance Foundation of Shaanxi Province (No. TD12-05), International Science and Technology Cooperation Project of

Shaanxi Province (2011KW-11) and the Graduate Innovation Foundation of Shaanxi University of Science and Technology.

References

[1] M. Boshta, M.O. Abou-Helal, D. Ghoneim, N.A. Mohsen, R.A. Zaghlool, The photocatalytic activity of sprayed $Zn_{1-x}Mg_xO$ thin films, Ceram. Int. 205 (2010) 271–274.

[2] S. Ekambaram, Yoichi Likubo, Akihiko Kudo, Combustion synthesis and photocatalytic properties of transition metal-incorporated ZnO, J. Alloys Compd. 433 (2007) 237–240.

[3] S. Suwanboon, P. Amornpitoksuk, N. Muensit, Dependence of photocatalytic activity on structural and optical properties of nanocrystalline ZnO powders, Ceram. Int. 37 (2011) 2247–2253.

[4] Jun bo Zhong, Jian Zhang Li, Yan Lu, Xi Yang He, Jun Zeng, Wei Hu, Yue Cheng Shen, Fabrication of Bi^{3+}-doped ZnO with enhanced photocatalytic performance, Appl. Surf. Sci. 258 (2012) 4929–4933.

[5] H. Benheal, M. Chaib, A. Leonard, S.D. Lambert, M. Crine, Photodegradation of phenol and benzoic acid by sol–gel synthesized alkali metal-doped ZnO, Mater. Sci. Semicond. Proc. 15 (2012) 264–269.

[6] J.H. Sun, S.Y. Dong, J.L. Feng, X.J. Yin, X.C. Zhao, Enhanced sunlight photocatalytic performance of Sn-doped ZnO for methylene blue degradation, J. Mol. Catal. A: Chem. 335 (2011) 145–150.

[7] M. Ahmad, Z.L. Hong, E. Ahmed, N.R. Khalid, A. Elhissi, W. Ahmad, Effect of fuel to oxidant molar ratio on the phoyocatalytic activity of ZnO nanopowders, Ceram. Int. 39 (2013) 3007–3015.

[8] S. Suwanboon, P. Amompitoksuk, A. Sukolral, N. Muensit, Optical and photocatalytic properties of La-doped ZnO nanoparticles prepared via precipitation and mechanical milling method, Ceram. Int. 39 (2013) 2811–2819.

[9] M. Ahmad, E. Ahmed, Y.W. Zhang, N.R. Khalid, J.F. Xu, M. Ullah, Z.L. Hong, Preparation of highly efficient Al-doped ZnO photocatalyst by combustion synthesis, Curr. Appl. Phys. 13 (2013) 697–704.

[10] F. Meng, J. Li, Z.L. Hong, M. Zhi, A. Sakla, C. Xiang, N.Q. Wu, Photocatalytic generation of hydrogen with visible-light nitrogen-doped lanthanum titanium oxides, Catal. Today 199 (2013) 48–52.

[11] J.C. Sin, S.M. Lam, K.T. Lee, A.R. Mohamed, Preparation and photocatalytic properties of visible light-driven sanmarium-doped ZnO nanorods, Ceram. Int. 39 (2013) 5833–5843.

[12] A.B. Patil, K.R. Patil, S.K. Pardeshi, Ecofriendly synthesis and solar photocatalytic activity of S-doped ZnO, J. Hazard. Mater. 183 (2010) 315–323.

[13] Ji-Zhou Kong, Ai-Dong Li, Hai-Fa Zhai, You-Pin Gong, Hui Li, Di Wu, Preparation, characterization of the Ta-doped ZnO nanoparticles and their photocatalytic activity under visible-light illumination, J. Solid State Chem. 182 (2009) 2061–2067.

[14] Changle Wu, Li Shen, Yong-Cai Zhang, Qingli Huang, Solvothermal synthesis of Cr-doped ZnO nanowires visible light-driven photocatalytic activity, Mater. Lett. 65 (2011) 1794–1796.

[15] Y. Zhang, W.F. Zhang, H.W. Zheng, Fabrication and photoluminescence properties of ZnO: Zn hollow microspheres, Scr. Mater. 57 (2007) 313–316.

[16] C. Ren, B. Yang, M. Wu, J. Xu, Z. Fu, Y. Lv, T. Guo, Y. Zhao, C. Zhu, Synthesis of Ag/ZnO nanorods array with enhanced photocatalytic performance, J. Hazard. Mater. 182 (2010) 123–129.

[17] Fatiha Barka-Bouaifel, Brigitte Sieber, Nacer Bezzi, Josef Benner, Pascal Roussel, Luc Boussekey, et al., Synthesis and photocatalytic activity of iodine-doped ZnO nanoflowers, J. Mater. Chem. 9 (2011) 10982–10989.

[18] N. Venkatachalam, M. Palanichamy, V. Murugesan, Sol–gel preparation and nanosize TiO_2: its photocatalytic performance, Mater. Chem. Phys. 15 (2007) 454–459.

[19] Elizabeth R. Carraway, Amy J. Hoffman, Michael R. Hoffmann, Photocatalytic oxidation of organic acids on quantum-sized semiconductor colloids, Environ. Sci. Technol. 28 (1994) 776.

[20] S. Sakthivel, B. Neppolian, M.V. Shankar, B. Arabindoo, M. Palanichamy, V. Murugesan, Solar photocatalytic degradation of azo dye: comparison of photocatalytic efficiency of ZnO and TiO_2, Sol. Energy Mater. Sol. Cells 30 (2003) 65–82.

[21] Xiaoqing Qiu, Liping Li, Jing Zheng, Junjie Liu, Xuefei Sun, Guangshe Li, Origin of the ehanced photocatalytic activities of semiconductors: a case study of ZnO doped with Mg^{2+}, J. Phys. Chem. C 112 (2008) 12242–12248.

[22] M. Bouloudenine, N. Viart, S. Colis, A. Dinia, Bulk $Zn_{1-x}Co_xO$ magnetic semiconductors prepared by hydrothermal technique, Chem. Phys. Lett. 11 (2004) 73–76.

[23] Edit Pal Viktoria Hornok, Albert Oszko, Imre Dekany, Hydrothermal synthesis of prism-like and flower-like ZnO and indium-doped ZnO structures, Colloids Surf. A 15 (2009) 1–9.

[24] Chao Xu, Lixin Cao, Ge Su, Wei Liu, Xiaofei Qu, Yaqin Yu, Preparation, characterization and photocatalytic activity of Co-doped ZnO powders, J. Alloy Compd. 14 (2010) 373–376.

[25] C.O. Kappe, Controlled microwave heating in modern organic synthesis, Angew. Chem. Int. Ed. 43 (2004) 6250.

[26] C.S. Cundy, The hydrothermal synthesis of zeolites: history and development the earliest days to the present time, Collect. Czech. Chem. Commun. 63 (1998) 1699.

[27] H. Katsuki, S. Furuta, S. Komarneni, Microwave versus conventional-hydrothermal synthesis of NaY zeolite, J. Porous Mater. 8 (2001) 5.

[28] T.H Lea, Q.D. Truong, T. Kimura, H. Li, C. Guo, S. Yin, T. Sato, Y.C. Ling, Synthesis of hierarchical porous ZnO microspheres and its photocatalytic deNO_x activity, Ceram. Int. 38 (2012) 5053–5059.

[29] S.M. Wang, Z.S. Yang, M.K. Lu, Y.Y. Zhou, G.J. Zhou, Z.F. Qiu, S.F. Wang, H.P. Zhang, A.Y. Zhang, A.Y. Zhang, Co-precipitation synthesis of hollow Zn_2SnO_4 spheres, Mater. Lett. 61 (2007) 3005–3008.

[30] Jianfeng Huang, Changkui Xia, Liyun Cao, Xierong Zeng, Facile microwave hydrothermal synthesis of zinc oxide one-dimensional nanostructure with three-dimensional morphology, Mater. Sci. Eng. B 150 (2008) 187–193.

[31] Ruh Ullah, Joydeep Dutta, Photocatalytic degradation of organic dyes with manganese-doped ZnO nanoparticles, J. Hazard. Mater. 156 (2008) 194–200.

[32] V. Stengl, S. Bakardjieva, N. Murafa, Preparation and photocatalytic activity of rare earth doped TiO_2 nanoparticles, Mater. Chem. Phys. 114 (2009) 217–226.

[33] S. Yilmaz, M. Parlak, S. Ozcan, M. Altunbas, E. McGlynn, E. Bacaksiz, Structural, optical and magnetic properties of Cr doped ZnO microrods prepared by spray pyrolysis method, Appl. Surf. Sci. 257 (2011) 9293–9298.

[34] Yiqiao Zhuo, Jianfeng Huang, Liyun Cao, Haibo Ouyang, Jianpeng Wu, Photocatalytic activity of snow-like Bi_2WO_6 microcrystalline for decomposition of Rhodamine B under natural sunlight irradiation, Mater. Lett. 90 (2013) 107–110.

[35] S. Anandan, A. Vinu, K.L.P. Sheeja Lovely, N. Gokulakrishnan, P. Srinivasu, T. Mori, V. Murugesan, V. Sivamurugan, K. Ariga, Photocatalytic activity of La-doped ZnO for the degradation of monocrotophos in aqueous suspension, J. Mol. Catal. A: Chem. 266 (2007) 149–157.

[36] Jin-Chung Sin, Sze-Mun Lam, Keat-Teong Lee, Abdul Rahman Mohamed, Fabrication of erbium-doped spherical-like ZnO hierarchical nanostructures with enhanced visible light-driven photocatalytic activity, Mater. Lett. 91 (2013) 1–4.

[37] Tiekun Jia, Weimin Wang, Fei Long, Zhengyi Fu, Hao Wang, Qingjie Zhang, Fabrication, characterization and photocatalytic activity of La-doped ZnO nanowires, J. Alloys Compd. 484 (2009) 410–415.

[38] Hongbo Fu, Chengshi Pan, Wenqing Yao, Yongfa Zhu, Visible-light-induced degradation of Rhodamine B by nanosized Bi_2WO_6, J. Phys. Chem. B 109 (2005) 22432.

[39] Rajneesh Mohan, Karthikeyan Krishnamoorthy, Sang-Jae Kim, Enhanced photocatalytic activity of Cu-doped ZnO nanorods, Solid State Commun. 152 (2012) 375–380.